

Load transfer and energy absorption in transversely compressed multi-walled carbon nanotubes

Xiaoming Chen¹ and Changhong Ke^{*1,2}

¹*Department of Mechanical Engineering, State University of New York at Binghamton, Binghamton, New York 13902, U.S.A.*

²*Materials Science and Engineering Program, State University of New York at Binghamton, Binghamton, New York 13902, U.S.A.*

(Received May 31, 2016, Revised May 24, 2017, Accepted May 25, 2017)

Abstract. We present a simple and easy-to-implement lumped stiffness model to elucidate the load transfer mechanism among all individual tube shells and intertube van der Waals (vdW) interactions in transversely compressed multi-walled carbon nanotubes (CNTs). Our model essentially enables theoretical predictions to be made of the relevant transverse mechanical behaviors of multi-walled tubes based on the transverse stiffness properties of single-walled tubes. We demonstrate the validity and accuracy of our model and theoretical predictions through a quantitative study of the transverse deformability of double- and triple-walled CNTs by utilizing our recently reported nanomechanical measurement data. Using the lumped stiffness model, we further evaluate the contribution of each individual tube shell and intertube vdW interaction to the strain energy absorption in the whole tube. Our results show that the innermost tube shell absorbs more strain energy than any other individual tube shells and intertube vdW interactions. Nanotubes of smaller number of walls and outer diameters are found to possess higher strain energy absorption capacities on both a per-volume and a per-weight basis. The proposed model and findings on the load transfer and the energy absorption in multi-walled CNTs directly contribute to a better understanding of their structural and mechanical properties and applications, and are also useful to study the transverse mechanical properties of other one-dimensional tubular nanostructures (e.g., boron nitride nanotubes).

Keywords: carbon nanotubes; transverse stiffness; load transfer; energy absorption

1. Introduction

The load-bearing and energy absorption capacities of carbon nanotubes (CNTs) are of great importance to their structural and physical properties and applications. From a structural point of view, multi-walled carbon nanotubes (MWCNTs) are composed of multiple concentric single-walled carbon nanotubes (SWCNTs) that are nested together via intertube van der Waals (vdW) interactions. For transversely compressed MWCNTs, the applied load is transferred fractionally and consecutively from the outermost tube shell all the way to the innermost shell via the intertube vdW interactions. Therefore, all the individual tube shells and intertube vdW interactions within

*Corresponding author, Associate Professor, E-mail: cke@binghamton.edu

the nanotube contribute to the sustaining of the external load and the absorption of the strain energy. Understanding the transverse intertube load transfer mechanism, in particular, the correlations on the load sustaining by each individual tube shell and intertube vdW interaction, is essential in pursuit of many of CNT-based material systems (e.g., CNT yarns and polymer nanocomposites) and their various structural applications. The transverse mechanical properties of SWCNTs (Barboza *et al.* 2009, Jiang *et al.* 2008, Li and Chou 2004, Tang *et al.* 2000, Wang *et al.* 2006, Yang and Li 2011, Zheng *et al.* 2012a, b) and MWCNTs (Cao *et al.* 2005, Muthaswami *et al.* 2007, Palaci *et al.* 2005, Shen *et al.* 2000, Xiao *et al.* 2006, Yu *et al.* 2000, Zheng *et al.* 2012c, d) have been extensively studied during the past decades using a variety of experimental and theoretical techniques. The transverse mechanical properties of MWCNTs have a strong dependence on its concentric tubular structure configurations. The transverse stiffness of MWCNTs increases with the number of tube walls, and decreases with the outer tube diameter. Prior research shows that the mechanical properties (e.g., elastic moduli) of SWCNTs have little dependence on the tube chirality (Lu 1997, Zhao *et al.* 2009), and the respective chiralities of the nested single-walled tubes within a MWCNT are largely randomized (Damjanović *et al.* 1999). Therefore, it is plausible that transverse mechanical properties of MWCNTs can be predicted based on those of individual SWCNTs, which possess the simplest tubular structural configurations. Double- and triple-walled CNTs (DWCNTs and TWCNTs) are two ideal model nanotube systems for this purpose due to their structural simplicity, making them relatively easier to handle both experimentally and theoretically. We want to highlight that such MWCNTs of low numbers of tube walls have recently attracted a great deal of attention due to their superior mechanical and electrical properties (Nam *et al.* 2016, Rakrak *et al.* 2016, Hajnayeb and Khadem 2015) as well as the unique freedom for surface modification of their outer tube shells while keeping their inner shells intact (Bouilly *et al.* 2011). They are being pursued for a variety of engineering applications, such as electronics (Green and Hersam 2011, Li *et al.* 2009, Morimoto *et al.* 2012), and transport (Popescu and Woods 2009) and sensing (Dong *et al.* 2008) devices.

In this paper, we present a simple and easy-to-implement lumped stiffness model to elucidate the load transfer mechanism among all individual tube shells and intertube vdW interactions in MWCNTs. Our model essentially enables theoretical predictions to be made of the relevant transverse mechanical behaviors of MWCNTs based on the transverse stiffness of SWCNTs. We demonstrate the validity and accuracy of our model and theoretical predictions through a quantitative study of the radial deformability of DWCNTs and TWCNTs by utilizing our recently reported experimental data obtained from atomic force microscopy (AFM)-based nanomechanical measurements. Using the lumped stiffness model, we further evaluate the contribution of each individual tube shell and intertube vdW interaction to the strain energy absorption in the whole tube. Our results remarkably reveal that the innermost tube shell absorbs more strain energy than any other individual tube shell and intertube vdW interaction. Nanotubes of smaller number of walls and outer diameters are found to possess higher strain energy absorption capacities on both a per-volume and a per-weight basis. Our proposed model and findings on the load transfer and energy absorption in MWCNTs directly contribute to a better understanding of structural and mechanical properties of CNTs and are useful to the functionality and performance optimization of their structural and mechanical applications (e.g., reinforcing fibers in nanocomposites). The proposed model is also useful in the study of the mechanical properties of other tubular nanostructures, such as boron nitride nanotubes (BNNTs). Because the transverse deformability of CNTs and BNNTs has a substantial influence on their electronic band-gap structures (Zheng *et al.* 2012b, Morimoto *et al.* 2012, Kinoshita and Ohno 2010, Crespi *et al.* 1997, Barboza *et al.* 2008,

Kim *et al.* 2001, Bai *et al.* 2007), our results are also useful in pursuit of the mechanical tuning of their electrical properties, thus impacting many of their electronics applications (Green and Hersam 2011, Li *et al.* 2009, Morimoto *et al.* 2012).

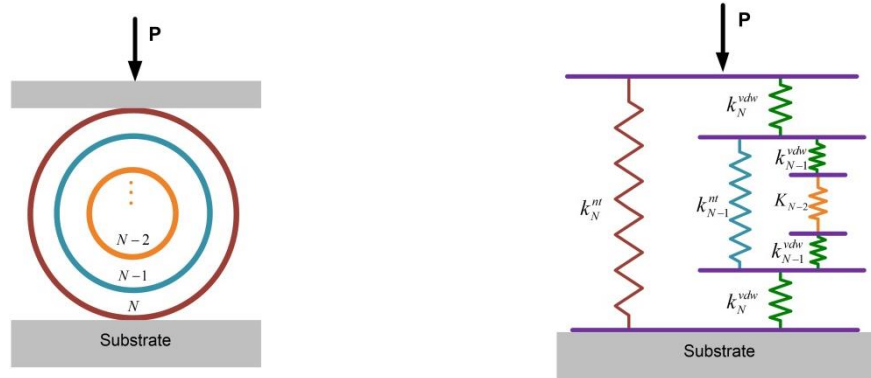
2. Results and discussion

2.1 Lumped stiffness model

Let us consider a generalized configuration of a transversely compressed MWCNT: a MWCNT of N tube shells and a length L staying between two rigid plates and compressed by a uniformly distributed line load with a total load magnitude P , whose undeformed cross-sectional configuration is schematically shown in Fig. 1(a). The N -walled nanotube can be generalized as a double-walled nanotube, in which its outermost tube shell and intertube vdW interaction are completely inherited, and its remaining inner tube subset, including $N-1$ tube shells and $N-2$ intertube vdW interactions, is lumped as the inner-wall tube. This generalization process can be repeatedly applied to the lumped inner-wall tube until it becomes the true single-walled tube. The external load P is applied on the surface of the outermost tube shell and is sustained accumulatively by each individual tube shell and intertube vdW interaction (Xiao *et al.* 2006), which are modeled as individual elastic springs with lumped stiffnesses as illustrated in Fig. 1(b). It is noted that each intertube vdW interaction appears twice in the cross-sectional deformation of the nanotube. The sustained load by each individual component can be determined from the iterative equilibrium conditions given as $P_i = p_i^{nt} + p_i^{vdw}$ and $p_i^{vdw} = p_{i-1}^{nt} + p_{i-1}^{vdw}$ for $i \in [1, N]$, where P_i and p_i^{nt} represent the forces applied on the surfaces of the i^{th} tube shell and the actual force sustained by the i^{th} tube shell, respectively; p_i^{vdw} represents the force sustained by the intertube vdW interaction between the i^{th} tube shell and its adjacent inner tube shell (*single occurrence here and thereafter*). It is clear that $P_N = P$, while $P_0 = 0$ and $p_1^{vdw} = 0$ for the case of SWCNTs (i.e., $N=1$). The cross-sectional deformation of the whole tube and its individual components can be easily identified from the iterative compatibility condition given as $\Delta_i = \delta_i^{nt} = \Delta_{i-1} + 2\delta_i^{vdw}$, where Δ and δ represent the respective deformations of the whole tube (or its inner tube subset) and individual tube shells/intertube vdW interactions, specified by their sub- and super-scripts. For intertube vdW interactions, δ_i^{vdw} refers to the intertube distance change between the i^{th} tube shell and its adjacent inner tube shell. Considering that the stiffness is the first order derivative of the force with respect to the deformation, the stiffness of the whole tube (or its inner tube subset) and its correlation with those of its individual components can be obtained from the following iterative relationship

$$K_i = k_i^{nt} + \frac{K_{i-1} \cdot k_i^{vdw}}{2K_{i-1} + k_i^{vdw}} \quad (1)$$

where K and k represent the respective stiffnesses of whole tube (or its inner tube subset) and its individual tube shells and intertube vdW interactions that are specified by their sub- and super-scripts. The transverse load versus deformation relationship for the whole tube can be obtained through integrating K_N , which is given as $P(\Delta_N) = \int K_N d\Delta_N$.



(a) Undeformed cross-section of an N -walled nanotube placed between two flat plates under a line load P (magnitude)
 (b) The lumped stiffness model for the transverse rigidity of the nanotube shown in (a)

Fig. 1 Schematic drawing of transversely compressed MWCNT and proposed stiffness model

Next, we look at the stiffness models for individual tube shells and intertube vdW interactions. Here, each single tube shell is simplified as an elastic cylinder in contact with a flat rigid substrate under a uniformly distributed compressive line load, and its transverse deformation can be estimated by well-established contact mechanics theories (Puttock and Thwaite 1969). It is noted that the flattening of the nanotube cross-section due to its vdW interaction with the contacting plates is neglected in all the contact mechanical models presented in this work (Hertel *et al.* 1998, Tang *et al.* 2005). The transverse deformation of the i^{th} tube shell under a line load with a total load magnitude p_i^{nt} and an acting length that is equal to the tube length L is expressed as (Puttock and Thwaite 1969)

$$\delta_i^{\text{nt}} = \frac{2p_i^{\text{nt}}}{L} \left(\frac{1 - \nu_{\text{nt}}^2}{\pi E_s^{\text{nt}}} \right) \left[1 + \log \left(\frac{2\pi E_s^{\text{nt}} L^3}{(1 - \nu_{\text{nt}}^2) p_i^{\text{nt}} D_i^{\text{nt}}} \right) \right] \quad (2)$$

where ν_{nt} and E_s^{nt} represent the Poisson's ratio of CNTs, and the effective radial elastic modulus of SWCNTs, respectively; D_i^{nt} represents the diameter of the i^{th} tube shell and is given as $D_i^{\text{nt}} = D_l + 2(i - 1)t$, in which D_l is the diameter of the innermost tube shell and $t = 0.34$ nm is the intertube distance in undeformed CNTs. The stiffness of each individual tube shell can be easily determined from Eq. (2) as $k_i^{\text{nt}} = \frac{\partial p_i^{\text{nt}}}{\partial \delta_i^{\text{nt}}}$.

When MWCNTs undertake transverse deformations, flat contacts occur between the adjacent nanotube shells, and the intertube distance decreases. Assuming that the vdW interactions at those non-flat contact regions remain unchanged, the actual load sustained by the vdW interaction is only contributed by its stiffness and the change of the intertube distance at the flat-contact regions. It is noted that Lennard-Jones potential has been widely used to study the vdW interaction in nanotube-based interfaces, such as the establishment of cohesive laws for nanotube-polymer and nanotube-substrate interfaces (Jiang *et al.* 2006, Lu *et al.* 2008, Zhou *et al.* 2007). The vdW

potential between two flat and infinite graphene sheets can be calculated using a continuum model based on Lennard-Jones potential, which is given as (Girifalco *et al.* 2000)

$$\Phi(\alpha) = -\frac{\Phi(Z_0)}{0.6} \left[\left(\frac{Z_0}{Z_0 - \alpha} \right)^4 - 0.4 \left(\frac{Z_0}{Z_0 - \alpha} \right)^{10} \right] \quad (3)$$

where $Z_0=0.341$ nm is the equilibrium distance between two infinite graphene sheets under force-free conditions, $\Phi(Z_0)=15.36$ meV/Å² is the vdW energy at the equilibrium, and α is the distance change from the equilibrium position. For the vdW interaction between the i^{th} tube shell and its adjacent inner tube shell with a flat-contact, its stiffness can be obtained through taking second-order differentiation of $\Phi(\alpha)$ with respect to α . Considering that $\alpha = \delta_i^{\text{vdw}}$, we have

$$k_i^{\text{vdw}} = \frac{20b_i L}{3} \frac{\Phi(Z_0)}{Z_0^2} \left[11 \left(\frac{Z_0}{Z_0 - \delta_i^{\text{vdw}}} \right)^{12} - 5 \left(\frac{Z_0}{Z_0 - \delta_i^{\text{vdw}}} \right)^6 \right] \quad (4)$$

where b_i is the width of the flat-contact, and is given as $b_i = \sqrt{(D_i^{\text{nt}})^2 - (D_i^{\text{nt}} - \delta_i^{\text{nt}})^2}$. Once the stiffnesses of individual tube shells and intertube vdW interactions are obtained, the stiffnesses of the whole tube and any of its nanotube subsets can be readily obtained by using Eq. (1).

2.2 Direct contact mechanics model for the whole tube

The transverse stiffnesses of MWCNTs are dependent not only on their structural configurations and material properties, but also on the applied load, which is exhibited by the nonlinear force-displacement relationship (Barboza *et al.* 2009, Muthaswami *et al.* 2007, Palaci *et al.* 2005). In order to facilitate the demonstration of the validity and accuracy of our proposed lumped stiffness model, we simplify MWCNTs as cylindrical elastic bodies whose cross-sectional structural configurations and transverse deformabilities can be characterized by their outer diameters D_N^{nt} and effective radial elastic moduli E_N^{nt} . We establish the transverse load-deformation relationship based on the same contact mechanics model as employed in the development of lumped stiffness model, which is referred as the *direct contact mechanics model* here and expressed as

$$\Delta_N = \frac{2P}{L} \left(\frac{1 - \nu_{\text{nt}}^2}{\pi E_N^{\text{nt}}} \right) \left[1 + \log \left(\frac{2\pi E_N^{\text{nt}} L^3}{(1 - \nu_{\text{nt}}^2) P \cdot D_N^{\text{nt}}} \right) \right] \quad (5)$$

It is noted that the effective radial elastic modulus is a physical quantity dependent on both geometrical configurations (e.g., diameter) and material elastic properties. The effective radial elastic moduli of single-, double- and triple-walled CNTs were recently reported by our group based on AFM-based nanomechanical compression measurements (Zheng *et al.* 2012a, c, e). In brief, the AFM compression tests were performed through controlling the tip of a pre-calibrated AFM cantilever to scan an individual nanotube on a silicon substrate in contact mode at a specified compressive load with the scanning direction perpendicular to the tube axis. The applied

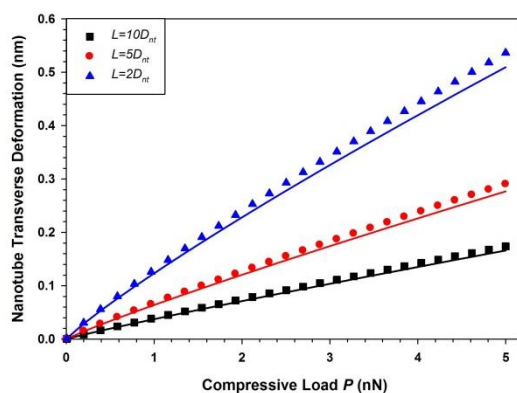


Fig. 2 The dependence of the nanotube transverse deformation profiles on the nanotube length for a DWCNT of 3.28 nm in outer diameter. The dotted lines represent the predictions based on the lumped stiffness model. The solid lines represent the deformation profiles calculated based on the direct contact mechanics model

compressive load and the transverse nanotube deformation were obtained through recording the vertical deflection of the employed AFM probe with a sub-angstrom resolution using laser-reflection schemes. It is noted that the cross-section of CNTs may experience a large deformation or even collapse when the compressed load is relatively large (Liu 2012). Our AFM measurements show that the transverse deformation of single to tripled CNTs were purely elastic under compressive loads of up to 5 nN, from which their effective radius moduli were obtained using Hertzian contact mechanics models. Therefore, the transverse deformability of single- to triple-walled CNTs and its dependence on their structural configuration were characterized by our AFM nanomechanical measurements. By using the direct contact mechanics model, the transverse deformation of MWCNTs can be calculated by using Eq. (5) based on their experimentally quantified effective radial modulus data.

2.3 Validation of the lumped stiffness model

We assess the validity and accuracy of our proposed lumped stiffness model through studying the transverse stiffness and force-deformation relationship of DWCNTs and TWCNTs. It is clear that the effective radial elastic moduli of SWCNTs are an essential parameter in the theoretical prediction of the radial rigidity of MWCNTs by using the lumped stiffness model. The measured effective radial elastic moduli of SWCNTs, which are displayed in Fig. 4 in ref. (Zheng *et al.* 2012a), can be satisfactorily approximated using a simple power-function fitting curve, given as

$$E_s^{nt} = 26.602 \left(D_s^{nt} \right)^{-1.931}$$

with an *R*-squared value of 0.98, in which E_s^{nt} and D_s^{nt} (the nanotube diameter) are in units of GPa and nm, respectively. Here we select six representative DWCNTs and TWCNTs from the tubes that were tested in our recent experimental studies of the transverse deformability of MWCNTs (Zheng *et al.* 2012c). Their outer diameters and the corresponding effective radial elastic moduli are 2.73 nm (11.2 GPa), 3.28 nm (7.1 GPa) and 4.01 nm (4.1 GPa) for DWCNTs, while 4.28 nm (7.6 GPa), 4.80 nm (4.9 GPa) and 5.16 nm (4.3 GPa) for TWCNTs.

Both Eqs. (2) and (5) show that the transverse stiffness of the nanotube depends on its length. To examine the effect of the nanotube length on its transverse deformation, we evaluate the

Table 1 Comparison of the nanotube transverse deformation profile on the nanotube length for a DWCNT of 3.28 nm in outer diameter (the applied compressive load $P = 5$ nN)

Nanotube length/outer diameter ratio	Transverse nanotube deformation (nm)		
	Lumped stiffness model	Direct contact mechanics model	Difference (%)
10	0.174	0.166	4.8
5	0.290	0.277	4.7
2	0.536	0.509	5.3

transverse deformation profiles of a DWCNT of 3.28 nm in outer diameter for three different nanotube lengths (namely 2, 5, and 10 times the nanotube outer diameter) based on the lumped stiffness model (Eq. (2)) and the direct contact mechanics model (Eq. (5)). A compressive load P of up to 5 nN is employed in the calculation. Please note that $\nu_m=0.17$ is employed in all the calculations (Yang and Li 2011). The results are presented in Fig. 2, and also listed in Table 1. The results clearly show that the nanotube length has a direct impact on the transverse deformation of the nanotube under the same compressive load. This observation is expected because the line load intensity decreases with the increase of the nanotube length under the same applied load. Our results also reveal that the difference between the results obtained using the lumped stiffness model and the direct contact mechanics model are quite close for all three examined nanotube lengths. This finding suggests that the nanotube length does not have a substantial impact on the evaluation of the accuracy and validity of the lumped stiffness model through its comparison with the results obtained from the direct contact mechanics model. Therefore, the nanotube length of 5 times the nanotube outer diameter is employed in all the calculations and results presented in the following sections.

The theoretically predicted transverse deformations for those selected DWCNTs and TWCNTs at applied loads of up to 5 nN are calculated using the aforementioned two models, which are found to be less than 9.1% of DWCNT outer diameters and less than 5.6% of TWCNT outer diameters. The results are presented as the solid and dotted plots in Fig. 3, which exhibit reasonably good agreements. The discrepancies of the calculated transverse deformations at $P = 5$ nN from these two models, which are listed in Table 2, are found to be within the range of negative 5.4% and 9.4% for three DWCNTs, while within the range of negative 7.4% and 7.6% for three TWCNTs. It is noted that, for both types of tubes, the discrepancy is mostly smaller for those tubes of larger diameters, and becomes larger as the tube diameter decreases. Beyond the assumptions and simplification in the establishment of our lumped stiffness model, the observed discrepancies may also reflect the accuracy uncertainties in the reported data on the effective radial moduli of SWCNTs and MWCNTs, including the uncertainties in the experimental measurements and the theoretical analysis. We want to point out that CNTs undergo complex deformation processes during our AFM-based nanomechanical compression tests, which involve bending, stretching, and rotation of the covalent C-C bonds in the nanotube. Therefore, the quantification of the effective radial modulus of CNTs based on simple contact mechanics models (e.g., the Hertzian contact mechanics model employed in our prior studies) may not fully account for their radial deformabilities. More precise modeling of the nanotube deformation using advanced computational approaches, such as finite element methods (FEM) and molecular dynamics (MD), is warranted for a more precise interpretation of the nanomechanical measurements, which is beyond the scope of this study. Nonetheless, the reasonable agreement between the predictions of

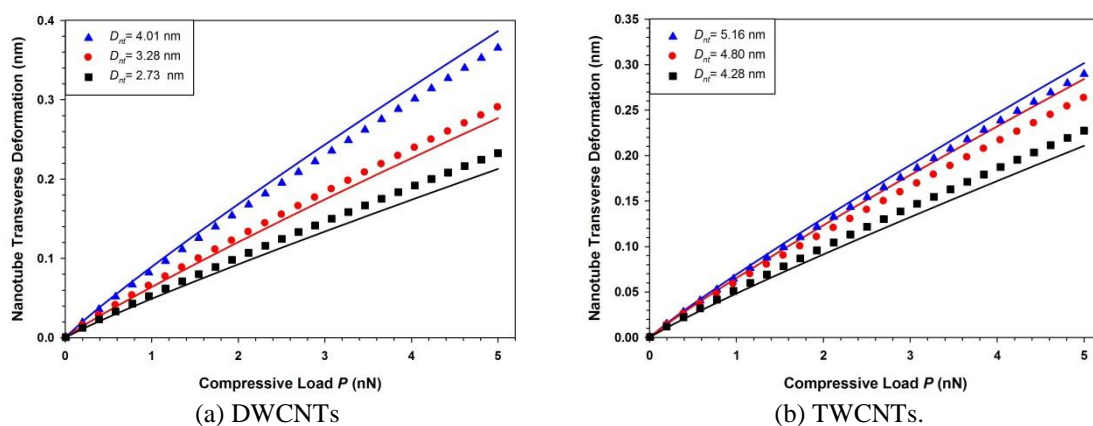


Fig. 3 The comparison of the nanotube transverse deformation profiles calculated based on the lumped stiffness model (dotted line) and the direct contact mechanics model (solid line) for three selected CNTs

Table 2 The comparison of the transverse deformation of nanotubes calculated based on the lumped stiffness model and the direct contact mechanics model for three selected DWCNTs and TWCNTs (the applied compressive load $P = 5$ nN)

Nanotube Type	Tube Shell Diameter (nm)			Transverse nanotube deformation (nm)		
	outer	middle	inner	Lumped stiffness model	Direct contact mechanics model	Absolute Difference (%)
DWCNTs	2.73	-	2.05	0.233	0.213	9.4
	3.28	-	2.60	0.290	0.277	4.7
	4.01	-	3.33	0.365	0.386	5.4
TWCNTs	4.28	3.60	2.92	0.227	0.211	7.6
	4.80	4.12	3.44	0.263	0.284	7.4
	5.16	4.48	3.80	0.290	0.302	4.0

the transverse deformation of MWCNTs as displayed in Fig. 3 suggests that the proposed lumped stiffness model is useful to elucidate the load transfer mechanism among individual tube shells and intertube vdW interactions. In particular, its simple and easy-to-implement formulation may enable or greatly facilitate the investigation of relevant physical and functionality properties that are originated from the transverse deformation of MWCNTs, such as the strain energy absorbed in the tube that is discussed in section 2.4.

Using the lumped stiffness model, the respective transverse stiffnesses of the whole tube and each of its individual tube shells and intertube vdW interactions are calculated for all the six selected tubes shown in Fig. 3. The results for two selected tubes are exhibited in Figs. 4(a)-(b). Our results on both tubes consistently show that the respective stiffnesses of the whole tubes and each of their components increase with the applied load, and the intertube vdW interaction(s) has a significantly higher stiffness than those of individual tube shells. For the TWCNT, it can be seen that the vdW interaction between the outer and the middle tube shells has a higher stiffness than the one between the middle and the inner tube shells. Table 3 lists the results for all the tubes under a compressive load of 5 nN. Our results consistently show that the stiffness of the whole tube and the respective stiffnesses of each individual tube shell decrease with the increase of the

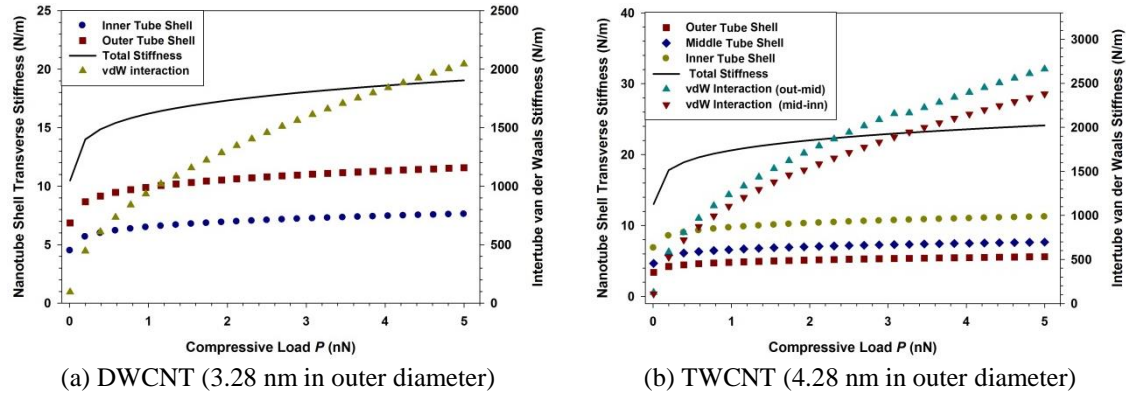


Fig. 4 The respective dependences of the theoretically predicted transverse stiffnesses of the whole tube and each individual tube shell/intertube vdW interaction on the compressive load for two selected tubes

Table 3 The theoretically predicted transverse stiffnesses of the whole tube and each of its nanotube shells and intertube van der Waals interaction layers for selected DWCNTs and TWCNTs. For all the calculations, the applied compressive load $P = 5$ nN, and the nanotube length is five times the nanotube outer diameter

Nanotube type	Tube Shell Diameter (nm)			Whole tube stiffness (N/m)	Tube shell stiffness (N/m)			Stiffness of intertube vdW interaction (N/m)	
	outer	middle	inner		outer	middle	inner	outer-middle	middle-inner
DWCNTs	2.73	-	2.05	23.8	9.0	-	15.1	1435.1	
	3.28	-	2.60	19.1	7.6	-	11.6	2043.9	
	4.01	-	3.33	15.1	6.3	-	8.9	2983.2	
TWCNTs	4.28	3.60	2.92	24.1	5.6	7.7	11.2	2662.2	2379.8
	4.80	4.12	3.44	20.8	5.0	6.7	9.3	3377.8	3080.7
	5.16	4.48	3.80	18.9	4.7	6.1	8.2	3957.3	3552.4

nanotube outer diameter, while the opposite trend is displayed for the stiffnesses of individual intertube vdW interactions. Our results suggest that, for CNTs with large outer diameters, their intertube vdW interactions can be reasonably assumed to be perfectly rigid. Thus, the stiffness of the whole can be simply estimated as the summation of the stiffnesses of all the individual tube shells. For example, for the DWCNT of 4.01 nm in outer diameter, the summation of the stiffnesses of two tube shells gives 15.2 N/m for $P=5$ nN, which is merely 0.7% higher than the stiffness of the whole tube (15.1 N/m). For the TWCNT of 5.16 nm in outer diameter, the summation of the stiffnesses of three tube shells gives 19 N/m for $P=5$ nN, which is merely 0.5% higher than the stiffness of the whole tube (18.9 N/m). It is noted that our findings on the stiffnesses of MWCNTs and their individual components agree with the theoretical results reported by Xiao *et al.* (2006) based on a continuum model in which the nanotube elastic radial stiffness was computed using a universal inter-atom potential among all the carbon atoms in the tube.

2.4 Energy absorption

Using the lumped stiffness model, we further examine the strain energy stored in transversely

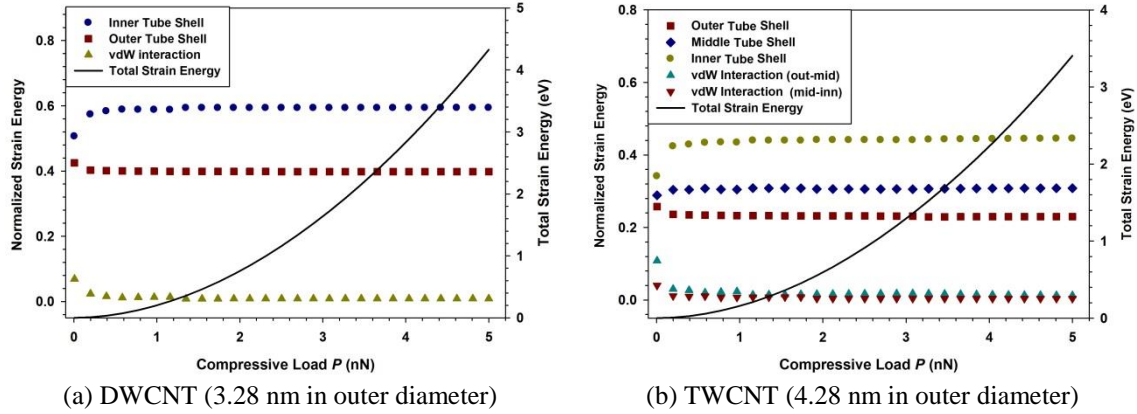


Fig. 5 The respective dependences of the theoretically predicted strain energy absorbed in the whole tube and each individual tube shell/intertube vdW interaction on the compressive load for two selected tubes

compressed MWCNTs and the respective energy absorption in each of their individual tube shells and intertube vdW interactions. Here we consider the compression of the nanotube by the line load as a quasi-static process. Thus, the strain energies stored in the whole tube and each of its individual components can be calculated as the areas under the respective load-displacement curves, and are given as $U_t = \int P_N d\Delta_N$ and $U_i^{nt(vdw)} = \int P_i^{nt(vdw)} d\delta_i^{nt(vdw)}$, respectively, in which its individual tube shells and intertube vdW interactions are specified by their superscripts. We calculate the energy absorption for all the examined tubes in the paper based on the lumped stiffness model. The solid curves in Figs. 5(a)-(b) show the computed total strain energies stored in a DWCNT of 3.28 nm in outer diameter and a TWCNT of 4.28 nm in outer diameter under a compressive load of up to 5 nN, respectively, while the respective contributions by individual tube shells and vdW interactions are displayed by the dotted curves. Table 4 lists the total strain energy and the contribution of each individual tube shell and vdW interaction layers for all the tubes under a compressive load of 5 nN. For both types of tubes, our results show that the total strain energy increases with the nanotube outer diameter as well as the applied load. It can be clearly seen from Figs. 5(a)-(b) that the contributions of individual inner and middle tube shells, on a normalized basis, first increase with the applied load, and then reach nearly saturated states when the applied load reaches about 4 nN. The strain energies stored in the outer tube shell and the van der Waals interaction layer(s) are found to undergo an opposite trend. Our results consistently show that the absorbed strain energy in tube shells are inversely correlated with their tube diameters and the innermost tube shell contributes the most to the energy absorption among all their individual tube shells and intertube vdW interactions. Meanwhile, for the tube type and diameter range investigated in our study, the energy absorbed by the outermost tube shell is still higher than any of the individual vdW interactions, and the difference increases with the nanotube outer diameter (see Table 4). Therefore, in the evaluation of the strain energy stored in transversely compressed CNTs, the intertube vdW interaction plays an important role only for tubes of small diameters, while it can be reasonably ignored for large-diameter tubes. Assuming that the intertube vdW interaction is perfectly rigid, the absorbed energy in each tube shell is essentially proportional to its stiffness, which is consistent with the data shown in Figs. 5(a)-(b).

We also evaluate the strain energy absorption capacities of both types of MWCNTs on both a

Table 4 The theoretically predicted strain energy absorbed in the whole tube and in each of its nanotube shells and intertube van der Waals interaction layers for selected DWCNTs and TWCNTs. For all the calculations, the applied compressive load $P = 5$ nN, and the nanotube length is five times the nanotube outer diameter

Nanotube type	Nanotube outer diameter (nm)	Total strain energy (eV)	Strain energy per unit volume (eV/nm^3) $\times 10^{-2}$	Strain energy per unit weight (eV/Kg) $\times 10^{22}$	Strain energy in tube shell (eV)			Strain energy in intertube vdW interaction layer (eV)	
					outer	middle	inner	outer-middle	middle-inner
DWCNTs	2.73	3.47	4.34	2.23	1.31	-	2.11	0.048	
	3.28	4.33	3.12	1.89	1.72	-	2.57	0.038	
	4.01	5.44	2.15	1.55	2.27	-	3.15	0.018	
TWCNTs	4.28	3.42	1.11	0.62	0.78	1.05	1.52	0.053	0.017
	4.80	3.97	0.90	0.56	0.95	1.25	1.71	0.044	0.016
	5.16	4.35	0.80	0.52	1.07	1.38	1.84	0.042	0.014

per-volume and a per-weight (mass) basis. The per-volume strain energy absorption is calculated as the total strain energy divided by the whole volume enclosed by the outer shell of the nanotube. The per-weight strain energy absorption is calculated as the total strain energy divided by the total mass in the tube that is a summation of the mass of each individual nanotube shell. The mass of individual carbon atom is about 1.99×10^{-26} kg. The graphene surface density of carbon atoms is $38/\text{nm}^2$. The mass density per unit area for a single nanotube shell is calculated as 7.57×10^{-25} kg/nm^2 . The strain energy absorption results, which are listed in Table 4, consistently show that double-walled tubes possess higher strain energy absorption capacities than triple-walled tubes on both a per-volume and a per-weight (mass) basis. For the same type of tubes, tubes of smaller outer diameter possess higher strain energy absorption capacities. The results and findings on the energy absorption in MWCNTs are of importance to their structural and mechanical applications. One such example is nanotube-based nano-composites, in which individual nanotubes are dispersed into matrix materials as reinforcing additives to improve their mechanical properties, such as modulus, strength, and toughness. Ultimately, the improvements of all these relevant mechanical properties are related to the energy absorption in the reinforcing nanotubes embedded into the matrix. Our findings suggest that it is of technological advantage to use tubes of smaller number of walls and outer diameters for strain energy absorption. Our proposed model and findings on the load transfer and energy absorption in MWCNTs are useful to the analysis of the energy absorption of CNTs inside elastic media and the failure mechanism of nanocomposites (Thostenson and Chou 2004), and thus are useful to the optimization of the functionality and performance of CNT-based nanocomposites.

3. Conclusions

In this paper, we present a lumped stiffness model to elucidate the load transfer mechanism in transversely compressed MWCNTs by taking into account the rigidities of individual tube shells and intertube vdW interactions and their nested tubular configurations. We demonstrate the

validity and accuracy of our model in the theoretical predictions of the transverse stiffness and deformation of DWCNTs and TWCNTs based on the recently reported experimental data obtained by AFM nanomechanical measurements. Using the proposed lumped stiffness model, we further evaluate the strain energy stored in transversely compressed CNTs and the respective contributions of each tube shell and intertube vdW interaction. Our results remarkably reveal that the innermost tube shell absorbs more strain energy than any other individual tube shells and intertube vdW interactions. Nanotubes of smaller number of walls and outer diameters possess higher strain energy absorption capacities. To the best of our knowledge, our proposed stiffness model is the first theoretical model that elucidates the load transfer mechanism in transversely compressed MWCNTs based on their experimentally measured transverse rigidities. Our proposed model and theoretical methodologies presented in this paper can be readily extended to the study of the load transfer and energy absorption in other types of MWCNTs as well as other types of nanotubes (e.g., boron nitride nanotubes). The results and findings on the load transfer and energy absorption in nanotubes contribute directly to a better understanding of structural and mechanical properties of tubular nanostructures, and are useful to the functionality and performance optimization of their structural and mechanical applications.

Acknowledgements

This work was supported by US Air Force Office of Scientific Research-low density materials program under Grant No. FA9550-15-1-0491.

References

- Bai, X., Golberg, D., Bando, Y., Zhi, C., Tang, C., Mitome, M. and Kurashima, K. (2007), "Deformation-driven electrical transport of individual boron nitride nanotubes", *Nano Lett.*, **7**(3), 632-637.
- Barboza, A.P.M., Chacham, H. and Neves, B.R.A. (2009), "Universal response of single-wall carbon nanotubes to radial compression", *Phys. Rev. Lett.*, **102**(2), 025501.
- Barboza, A.P.M., Gomes, A.P., Archanjo, B.S., Araujo, P.T., Jorio, A., Ferlauto, A.S., Mazzoni, M.S.C., Chacham, H. and Neves, B.R.A. (2008), "Deformation induced semiconductor-metal transition in single wall carbon nanotubes probed by electric force microscopy", *Phys. Rev. Lett.*, **100**(25), 256804.
- Bouilly, D., Cabana, J., Meunier, F., Desjardins-Carriere, M., Lapointe, F., Gagnon, P., Larouche, F.L., Adam, E., Paillet, M. and Martel, R. (2011), "Wall-selective probing of double-walled carbon nanotubes using covalent functionalization RID G-7589-2011", *Acs Nano*, **5**(6), 4927-4934.
- Cao, G., Tang, Y. and Chen, X. (2005), "Elastic properties of carbon nanotubes in the radial direction", *Proceedings of the Institution of Mechanical Engineers, Part N: Journal of Nanoengineering and Nanosystems*, **219**(2), 73-88.
- Crespi, V.H., Cohen, M.L. and Rubio, A. (1997), "In situ band gap engineering of carbon nanotubes", *Phys. Rev. Lett.*, **79**(11), 2093-2096.
- Damnjanović, M., Milošević, I., Vuković, T. and Sredanović, R. (1999), "Full symmetry, optical activity, and potentials of single-wall and multiwall nanotubes", *Phys. Rev. B*, **60**(4), 2728-2739.
- Dong, X., Fu, D., Xu, Y., Wei, J., Shi, Y., Chen, P. and Li, L.J. (2008), "Label-free electronic detection of DNA using simple double-walled carbon nanotube resistors", *J. Phys. Chem. C*, **112**(26), 9891-9895.
- Girifalco, L.A., Hodak, M. and Lee, R.S. (2000), "Carbon nanotubes, buckyballs, ropes, and a universal graphitic potential", *Phys. Rev. B*, **62**(19), 13104-13110.
- Green, A.A. and Hersam, M.C. (2011), "Properties and application of double-walled carbon nanotubes

- sorted by outer-wall electronic type”, *ACS Nano*, **5**(2), 1459-1467.
- Hajnayeb, A. and Khadem, S.E. (2015), “An analytical study on the nonlinear vibration of a double walled carbon nanotube”, *Struct. Eng. Mech.*, **54**(5), 987-998.
- Hertel, T., Walkup, R.E. and Avouris, P. (1998), “Deformation of carbon nanotubes by surface van der Waals forces”, *Phys. Rev. B*, **58**(20), 13870-13873.
- Jiang, L.Y., Huang, Y., Jiang, H., Ravichandran, G., Gao, H., Hwang, K.C. and Liu, B. (2006), “A cohesive law for carbon nanotube/polymer interfaces based on the van der waals force”, *J. Mech. Phys. Sol.*, **54**(11), 2436-2452.
- Jiang, Y.Y., Zhou, W., Kim, T., Huang, Y. and Zuo, J.M. (2008), “Measurement of radial deformation of single-wall carbon nanotubes induced by intertube van der waals forces”, *Phys. Rev. B*, **77**(15), 153405.
- Kim, Y.H., Chang, K.J. and Louie, S.G. (2001), “Electronic structure of radially deformed BN and BC3 nanotubes”, *Phys. Rev. B*, **63**(20), 205408.
- Kinoshita, Y. and Ohno, N. (2010), “Electronic structures of boron nitride nanotubes subjected to tension, torsion, and flattening: A first-principles DFT study”, *Phys. Rev. B*, **82**(8), 085433.
- Li, C. and Chou, T.W. (2004), “Elastic properties of single-walled carbon nanotubes in transverse directions”, *Phys. Rev. B*, **69**(7), 073401.
- Li, Y., Hatakeyama, R., Oohara, W. and Kaneko, T. (2009), “Formation of p-n junction in double-walled carbon nanotubes based on heteromaterial encapsulation”, *Appl. Phys. Expr.*, **2**(9), 095005.
- Liu, J. (2012), “Explicit solutions for a SWCNT collapse”, *Arch. Appl. Mech.*, **82**(6), 767-776.
- Lu, J.P. (1997), “Elastic properties of carbon nanotubes and nanoropes”, *Phys. Rev. Lett.*, **79**(7), 1297-1300.
- Lu, W.B., Wu, J., Song, J., Hwang, K.C., Jiang, L.Y. and Huang, Y. (2008), “A cohesive law for interfaces between multi-wall carbon nanotubes and polymers due to the van der waals interactions”, *Comput. Meth. Appl. Mech. Eng.*, **197**(41-42), 3261-3267.
- Morimoto, T., Kuno, A., Yajima, S., Ishibashi, K., Tsuchiya, K. and Yajima, H. (2012), “Effective energy gap of the double-walled carbon nanotubes with field effect transistors ambipolar characteristics”, *Appl. Phys. Lett.*, **100**(4), 043107.
- Muthaswami, L., Zheng, Y., Vajtai, R., Shekhawat, G., Ajayan, P. and Geer, R.E. (2007), “Variation of radial elasticity in multiwalled carbon nanotubes”, *Nano Lett.*, **7**(12), 3891-3894.
- Nam, I.W., Souri, H. and Lee, H.K. (2016), “Percolation threshold and piezoresistive response of multi-wall carbon nanotube/cement composites”, *Smart Struct. Syst.*, **18**(2), 217-231.
- Palaci, I., Fedrigo, S., Brune, H., Klinke, C., Chen, M. and Riedo, E. (2005), “Radial elasticity of multiwalled carbon nanotubes”, *Phys. Rev. Lett.*, **94**(17), 175502.
- Popescu, A. and Woods, L.M. (2009), “Telescopic hot double wall carbon nanotube for nanolithography”, *Appl. Phys. Lett.*, **95**(20), 203507.
- Puttock, M.J. and Thwaite, E.G. (1969), *Elastic Compression of Spheres and Cylinders at Point and Line Contact*, Commonwealth Scientific and Industrial Research Organization, Melbourne, Australia.
- Rakrak, K., Zidour, M., Heireche, H., Bousahla, A.A. and Chermi, A. (2016), “Free vibration analysis of chiral double-walled carbon nanotube using non-local elasticity theory”, *Adv. Nano Res.*, **4**(1), 31-44.
- Shen, W., Jiang, B., Han, B.S. and Xie, S. (2000), “Investigation of the radial compression of carbon nanotubes with a scanning probe microscope”, *Phys. Rev. Lett.*, **84**(16), 3634-3637.
- Tang, J., Qin, L.C., Sasaki, T., Yudasaka, M., Matsushita, A. and Iijima, S. (2000), “Compressibility and polygonization of single-walled carbon nanotubes under hydrostatic pressure”, *Phys. Rev. Lett.*, **85**(9), 1887-1889.
- Tang, T., Jagota, A. and Hui, C.Y. (2005), “Adhesion between single-walled carbon nanotubes”, *J. Appl. Phys.*, **97**(7), 074304.
- Thostenson, C. (2004), “Nanotube buckling in aligned multi-wall carbon nanotube composites”, *Carbon*, **42**(14), 3015-3018.
- Wang, H.Y., Zhao, M. and Mao, S.X. (2006), “Radial moduli of individual single-walled carbon nanotubes with and without electric current flow”, *Appl. Phys. Lett.*, **89**(21), 211906.
- Xiao, J., Lopatnikov, S., Gama, B. and Gillespie, J. (2006), “Nanomechanics on the deformation of single- and multi-walled carbon nanotubes under radial pressure”, *Mater. Sci. Eng. a-Struct. Mater. Propert.*

- Microstruct. Process.*, **416**(1-2), 192-204.
- Yang, Y.H. and Li, W.Z. (2011), "Radial elasticity of single-walled carbon nanotube measured by atomic force microscopy", *Appl. Phys. Lett.*, **98**(4), 041901.
- Yu, M.F., Kowalewski, T. and Ruoff, R.S. (2000), "Investigation of the radial deformability of individual carbon nanotubes under controlled indentation force", *Phys. Rev. Lett.*, **85**(7), 1456-1459.
- Zhao, H., Min, K. and Aluru, N.R. (2009), "Size and chirality dependent elastic properties of graphene nanoribbons under uniaxial tension", *Nano Lett.*, **9**(8), 3012-3015.
- Zheng, M., Chen, X., Bae, I.T., Ke, C., Park, C., Smith, M.W. and Jordan, K. (2012a), "Radial mechanical properties of single-walled boron nitride nanotubes", *Small*, **8**(1), 116-121.
- Zheng, M., Zou, L.F., Wang, H., Park, C. and Ke, C. (2012b), "Engineering radial deformations in single-walled carbon and boron nitride nanotubes using ultrathin nanomembranes", *ACS Nano*, **6**(2), 1814-1822.
- Zheng, M., Chen, X., Park, C. and Ke, C. (2012c), "Radial deformability of carbon and boron nitride nanotubes", *Proceeding of the 23rd International Congress of Theoretical and Applied Mechanics*, Beijing, China, August.
- Zheng, M., Zou, L., Wang, H., Park, C. and Ke, C. (2012d), "Quantifying the transverse deformability of double-walled carbon and boron nitride nanotubes using an ultrathin nanomembrane covering scheme", *J. Appl. Phys.*, **112**(10), 104318.
- Zheng, M., Ke, C., Bae, I.T., Park, C., Smith, M.W. and Jordan, K. (2012e), "Radial elasticity of multi-walled boron nitride nanotubes", *Nanotechnol.*, **23**(9), 095703.
- Zhou, W., Huang, Y., Liu, B., Wu, J., Hwang, K.C. and Wei, B.Q. (2007), "Adhesion between carbon nanotubes and substrate: Mimicking the gecko foothair", *Nano*, **2**(3), 175-179.